Triplet correlation functions for hard spheres: Comparison of different approaches

Bernhard Bildstein and Gerhard Kahl
Institut für Theoretische Physik, Technische Universität Wien, Wiedner Hauptstraße 8-10, A-1040 Wien, Austria
(Received 13 July 1992; revised manuscript received 29 October 1992)

We present numerical results of a comparison between several approximations for the determination of the triplet correlation functions of a simple liquid, which have been proposed during recent years; the system we have considered is a simple hard-sphere system. Two of the methods (one proposed by Barrat, Hansen, and Pastore [Phys. Rev. Lett. **58**, 2075 (1987); Mol. Phys. **63**, 747 (1988)], and the other one based on a formal density expansion of the triplet distribution function) are purely numerical; the other two methods are based on a density-functional theory (reproducing both thermodynamics and pair structure of the Wertheim-Thiele description of hard spheres) and provide for this special system analytic expressions of the triplet direct correlation function in q space. If the triplet configurations are not too close (i.e., at most one direct contact between the spheres), we find good agreement between the different methods; this is quite remarkable since these approximations have completely different conceptual origins. If, however, the three particles form configurations with rather short interparticle distances the differences in the results may become quite substantial.

PACS number(s): 61.20.Gy, 61.20.Ne

I. INTRODUCTION

Attempts of liquid-state physicists to determine the triplet correlation function (TCF's) of a simple liquid date back to the end of the 1950s; ever since, several approaches have been proposed to solve this problem [1–13]. While nowadays the pair correlation functions of a simple liquid can be determined in a very consistent way (thanks to a large number of rather sophisticated methods which have been proposed during the past thirty years and which have been discussed widely in literature, cf., e.g., Hansen and McDonald [14]), we are in the triplet case at the beginning; this is, to a large extent, due to the mathematical and computational complexity of the problem. In the pair case we have arrived at a level where *different* methods yield—for a great variety of potentials of simple liquids—both for thermodynamics and structure results which agree within numerical accuracy, even though these methods originate from completely different roots (as, e.g., computer simulations, perturbation theories, or integral-equation techniques; cf., e.g., Talbot *et al.* [15]). The increasing interest in TCF's during the past years may be partly attributed to the actual computational power of supercomputers: realization of several approaches which were proposed already some time ago and then were too time consuming has now come into reach; nevertheless, the determination of the *full* triplet structure is—in contrast to the pair structure—still far from being a standard problem: according to the information available in the literature and according to our experience the accurate determination of the TCF's from this contribution is still a time- and storage-consuming problem both for numerical [5, 16] and simulation methods [9, 17]. Therefore it is not surprising that numerical data on the triplet structure determined by the different methods mentioned above are still rare. This holds especially for computer simulation data, a fact which is even more deplorable since in liquid-state physics such results are indispensable to check the realiability of a proposed method.

Since only a few computer simulation data of the triplet structure of simple liquids are available [9, 18], we have devoted this contribution to a study in which different *numerical* methods are compared. Even though a comparison with simulation data would be a more stringent test of the reliability of a numerical method, this study might also give—for lack of computer simulation data—an idea of how consistent the picture is which emerges from present-day methods for the determination of TCF's. The system we have chosen is described by the most simple model interaction available, i.e., by a hard-sphere (HS) potential, which still plays—despite of its simplicity—a key-role in liquid-state physics, e.g., as a reference system in perturbation theories or integral-equation techniques when determining thermodynamics and pair structure of simple liquids; perhaps, one day this system might serve as well as a reference system for the triplet structure of liquids with soft interactions, if respective theories are developed. The choice for this system is justified by the facts that (i) HS's are characterized by one single parameter (the packing fraction η), thus facilitating both the scanning of the parameter space and the presentation of the data and (ii) both pair structure and thermodynamics (which, as we will see, serve as input for the different methods treated here) are available in analytic expressions, based on the analytic solution of the Percus-Yevick (PY) equation for HS's [19]. (Furthermore, the knowledge of these analytic expressions also allows in some of the methods treated here an analytic representation of the TCF's. In order to preserve this advantage we do not take into account other expressions [20] which were derived to parametrize the pair structure

of HS obtained in computer experiments.)

In this study we have considered four methods: the first approximation, due to Barrat, Hansen, and Pastore (BHP) [3, 4], is based on a factorization ansatz of the pair direct CF (PDCF) $c(r)$, which is the only input required. In our case, we know this function from the Wertheim-Thiele solution [19]. From the factor-function $t(r)$ the triplet distribution function (TDF) may be determined via the generalized Ornstein-Zernike (OZ) relation [4, 21]. The second method, based on work by Abe [22] and Salpeter [23] starts from a formal density expansion of the TDF: to lowest order we recover the well-known Kirkwood superposition approximation (SA) [24], with correcting terms expressed as $h^{(2)}$-bond diagrams [$h^{(2)}(r)$ is the total CF], which become rapidly more complicated as the order of the expansion rises. The other two methods are based on density-functional (DF) theory for the free energy of inhomogeneous liquids (for an overview see, e.g., Evans [25]). The excess free-energy functional is constructed to reproduce both thermodynamics and pair structure of the homogeneous HS liquid in the framework of the PY theory; the n-particle CF is then obtained from the nth-order functional derivative of this functional with respect to the density. Among the methods proposed in literature [8–13] we have chosen those due to Denton and Ashcroft (DA) [11] and Kierlik and Rosinberg (KR) [10]. For both of them the energy functional is an analytic expression for this specific system; hence the triplet DCF (TDCF) may be calculated for the HS system in q space analytically. The TDF, as a function in r space, is again obtained via the generalized OZ relation [4, 21]. Several methods based on DF theory [10, 13] have already been compared to recent, very accurate computer experiments by Rosenfeld, Levesque, and Weis [9] in q space; we find, however, from these results that none of these methods is able to provide a convincing overall agreement, which would confirm one of them as being definitively superior to the others.

In the first part of this study we have investigated the angular dependence of the results: we have compared the above-mentioned methods for two different systems characterized by $\eta = 0.3$ and 0.45, considering for both cases six different triplet configurations (the triangles being defined by two fixed sides and an angle which varies between 0 and π). These configurations are rather general ones, i.e., triangles with at most one direct contact between the spheres, i.e., not too close structures. We find in all these cases—if we leave for the moment the pure SA out of consideration—an astonishingly good agreement, which is the more surprising as all the methods originate from different concepts. In the study on the radial dependence we consider both isosceles and general triangles (with one side being twice as large as the other and values for the enclosed angle of $\pi/3$, $\pi/2$, and $2\pi/3$). The results of this part of the study lead to the same conclusions as obtained from the angular dependence. In a final comparison we have considered configurations of "rolling contact," for which (not too recent) computer experiments exist [18]; they are, in turn, in extremely good agreement with a method recently proposed by Attard [5]. Compared to the general configurations mentioned above the situation is now somewhat different: obviously these geometries are more sensitive to the different nature of the methods (however, qualitative agreement is still preserved). This situation may be compared to the pair case where, e.g., PY and hypernetted-chain (HNC) approximations yield strongly different results for the CF's at contact, whereas at longer distances (which correspond in the triplet case to larger triangle configurations) these differences are not so extreme.

The paper is organized as follows. In Sec. II we present briefly the different methods used, leaving, however, a closer description to the respective publications. Section III presents our results and the paper is closed with concluding remarks. An Appendix contains numerical details of the actual calculations.

II. METHODS

A. General remarks

Henceforward we consider three particles (1, 2, and 3) which form a triangle: its sides will be denoted by r, s, and t. All distances will be given in units of the hard-core diameter, which is assumed to be unity.

The different CF's in q and r space are related via the Ornstein-Zernike relations [4, 21], which read in q space for the two particle

$$\hat{h}^{(2)}(q) = \hat{c}^{(2)}(q) + \rho \hat{h}^{(2)}(q)\hat{c}^{(2)}(q) \tag{1}$$

and for the three particle (TOZ) case

$$\hat{h}^{(3)}(q_1, q_2, |\mathbf{q}_1 + \mathbf{q}_2|) = \hat{h}^{(2)}(q_1)\hat{h}^{(2)}(q_2) + \hat{h}^{(2)}(q_1)\hat{h}^{(2)}(|\mathbf{q}_1 + \mathbf{q}_2|) + \hat{h}^{(2)}(q_2)\hat{h}^{(2)}(|\mathbf{q}_1 + \mathbf{q}_2|) + \frac{\hat{c}^{(3)}(q_1, q_2, |\mathbf{q}_1 + \mathbf{q}_2|) + \rho\hat{c}^{(2)}(q_1)\hat{c}^{(2)}(q_2)\hat{c}^{(2)}(|\mathbf{q}_1 + \mathbf{q}_2|)}{[1 - \rho\hat{c}^{(2)}(q_1)][1 - \rho\hat{c}^{(2)}(q_2)][1 - \rho\hat{c}^{(2)}(|\mathbf{q}_1 + \mathbf{q}_2|)]}. \tag{2}$$

$\hat{c}^{(2)}(q)$ and $\hat{h}^{(2)}(q)$ [$\hat{c}^{(3)}(q, q', q'')$ and $\hat{h}^{(3)}(q, q', q'')$] are the pair (triplet) direct and total CF's. Henceforward carets represent Fourier transforms (FT's), which are defined via

$$f(\mathbf{r}) = \frac{1}{(2\pi)^3}\int e^{i\mathbf{q}\cdot\mathbf{r}}\hat{f}(\mathbf{q})d\,\mathbf{q},$$
$$f(\mathbf{r}, \mathbf{r}') = \frac{1}{(2\pi)^6}\int e^{i\mathbf{q}\cdot\mathbf{r}}e^{i\mathbf{q}'\cdot\mathbf{r}'}\hat{f}(\mathbf{q}, \mathbf{q}')d\,\mathbf{q}d\,\mathbf{q}'. \tag{3}$$

We want to point out that (2) is only one formulation among several other equivalent expressions for the TOZ [21]. $h^{(3)}(r, s, t)$ is related to the TDF $g^{(3)}(r, s, t)$ via

$$h^{(3)}(r, s, t) = g^{(3)}(r, s, t) - h^{(2)}(r) - h^{(2)}(s) - h^{(2)}(t) - 1. \tag{4}$$

In the following we will briefly describe the different

methods used (and implemented) for this study, leaving, however, the details to the original papers. The Appendix contains numerical parameters of the actual calculations.

B. Methods

The first approximation is based on a formal density expansion of $g^{(3)}(r,s,t)$ due to Salpeter [23] and Abe [22]. The leading factor in this expansion is the Kirkwood SA [24]

$$g^{(3)}(r,s,t) = g(r)g(s)g(t). \tag{5}$$

$g(r) = g^{(2)}(r) = h^{(2)}(r) + 1$ is the pair distribution functions (PDF). The correcting terms to the SA (5) are ordered in powers of the number density ρ and are represented by cluster integrals whose bonds are Mayer f bonds ($f(r) = \exp[-\beta v(r)] - 1$). Stell [1] has used a topological reduction technique, replacing the f bonds by $h^{(2)}$ bonds which results in a drastic reduction of the number of required $h^{(2)}$-bond diagrams. Finally the expansion can be written as

$$g^{(3)}(r,s,t) = g(r)g(s)g(t)\exp\left(\sum_i \rho^i \tau_i(r,s,t;\rho)\right), \tag{6}$$

where $\tau_1(r,s,t;\rho)$ and $\tau_2(r,s,t;\rho)$ may be conveniently expressed by diagrams where lines now represent $h^{(2)}$ bonds:

$\tau_1(r,s,t;\rho) =$ 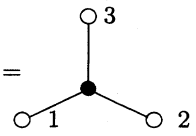

, (7)

$\tau_2(r,s,t;\rho) =$ 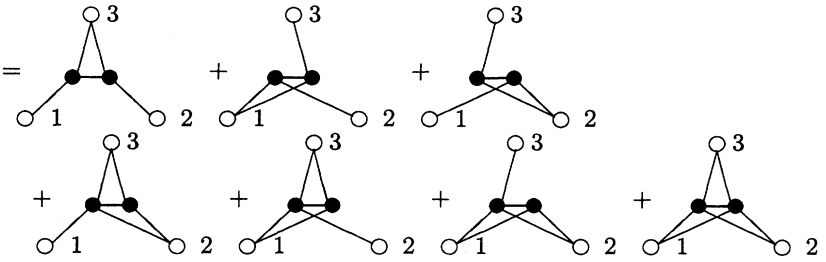

. (8)

The open, unweighted circles (root points) represent the three particles (i=1, 2, 3) at positions $\mathbf{r}_i$ ($r = |\mathbf{r}_{12}| = |\mathbf{r}_1 - \mathbf{r}_2|, s = |\mathbf{r}_{13}| = |\mathbf{r}_1 - \mathbf{r}_3|, t = |\mathbf{r}_{23}| = |\mathbf{r}_2 - \mathbf{r}_3|$); the full, ρ-weighted circles (field points) represent particles over which integrations are performed (cf., e.g., Hansen and McDonald [14]). Including the first (second) order term in (6) the respective approximations will be denoted as SA1 (SA2). Going beyond second order in (6) is completely hopeless: $\tau_3(r,s,t)$ contains ~ 100 diagrams, being much more complicated than those of (8). The diagrams in (7) and (8) are conveniently evaluated by means of a Legendre-expansion technique [26] in terms of $x = \cos\vartheta$, where ϑ is, e.g., the angle between $\mathbf{r}_{12}$ and $\mathbf{r}_{13}$. The only input required is the function $h^{(2)}(r)$ of the HS system which has been obtained via a semianalytic expression [27]: it allows an accurate evaluation of this function up to $r = 7$ (where, even for higher densities, $h^{(2)}(r)$ is already practically zero).

BHP proposed the following ansatz for the TDCF in r space [3, 4]:

$$c^{(3)}(r,s,t) = t(r)t(s)t(t), \tag{9}$$

where the function $t(r)$ is determined from the relation

$$\frac{\partial c^{(2)}(r)}{\partial \rho} = t(r)\int t(r')t(|\mathbf{r} - \mathbf{r}'|)\mathrm{d}\mathbf{r}'. \tag{10}$$

This equation is nothing else but the exact relation between $c^{(2)}$ and $c^{(3)}$ obtained from DF formalism [25] (see below),

$$\frac{\partial c^{(2)}(r)}{\partial \rho} = \int c^{(3)}(r,r',|\mathbf{r} - \mathbf{r}'|)\mathrm{d}\mathbf{r}'. \tag{11}$$

One may show that $\hat{c}^{(3)}(q,q',q'')$ agrees with the exact TDCF at least up to second order in the wave numbers [3, 4]. Using for $c^{(2)}(r)$ the analytic expression due to Wertheim and Thiele [19], $t(r)$ has been obtained from a numerical solution of (10) [28]; $c^{(3)}$ is then recovered via (9).

The other two methods treated here are based on DF theory for inhomogeneous fluids [25], where the excess Helmholtz free energy $F_{\mathrm{ex}}[\rho(r)]$ is considered as a functional of the inhomogeneous density $\rho(\mathbf{r})$. In order to design a model for $F_{\mathrm{ex}}[\rho(r)]$ which takes into account the main characteristics of the real system, several approaches have been proposed, as the local density approximation (LDA) (eventually including nonlocal corrections), the smoothed density approximation (SDA) [29], or the weighted density approximation (WDA) [30].

The methods used here are based on the WDA: while the LDA assumes that $\rho(r)$ varies in the range of the interaction only smoothly, the WDA introduces the nonlocality of the free energy functional via a smoothed den-

sity $\bar{\rho}(r)$ (corresponding to a mean density around a particle in $\mathbf{r}$ in a volume related to the range of the interaction):

$$\bar{\rho}(r) = \int d\,\mathbf{r}'\rho(\mathbf{r}')w(|\,\mathbf{r}-\mathbf{r}'\,|;\rho). \tag{12}$$

$w(\mathbf{r};\rho)$ is a (possibly density-dependent) weight function.

The nth-order correlation functions of the *homogeneous* system are related to the nth-order functional derivative of the excess Helmholtz free energy with respect to $\rho(r)$ and then taking the uniform limit $\rho(r) \to \rho$ [25]:

$$c^{(n)}(\mathbf{r}_1,\ldots,\mathbf{r}_n;\rho) = -\frac{\beta\delta^n F_{\mathrm{ex}}[\rho(r)]}{\delta\rho(\mathbf{r}_1)\cdots\delta\rho(\mathbf{r}_n)}\bigg|_{\rho(r)=\rho}. \tag{13}$$

The functional $F_{\mathrm{ex}}[\rho(r)]$ is constructed to reproduce, within this formalism, known properties of the homogeneous liquid such as, e.g., the excess free energy per particle and/or the PDCF. An analytical determination of F_{ex} is not always guaranteed (as, e.g., in the case of the SDA [29] or the WDA of Curtin and Ashcroft [30]). Furthermore, the determination of the weight function $w(\mathbf{r};\rho)$ may become in some cases a cumbersome numerical task [30].

The two approximations treated here introduce the WDA at different levels.

Kierlik and Rosinberg [10] introduce the WDA at the level of $F_{\mathrm{ex}}[\rho(r)]$

$$F_{\mathrm{ex}}[\rho] = \int d\,\mathbf{r}\,\phi(\bar{\rho}(r)), \tag{14}$$

where $\bar{\rho}$ is a weighted average over the physical density ρ [cf. (12)]. In contrast to Denton and Ashcroft (see below), KR assume $w(r)$ to be density independent; besides that, $w(r)$ is not uniquely determined (cf. discussion in Ref. [10]). Using the weight function proposed by KR, the TDCF may be expressed analytically (we do not reproduce the somewhat lengthy expressions here).

Denton and Ashcroft [11, 12] make a weighted density approximation for the one particle DCF

$$c^{(1)}(\mathbf{r};[\rho]) = c_0^{(1)}[\bar{\rho}(\mathbf{r})], \tag{15}$$

where

$$\bar{\rho}(\mathbf{r}) = \int \mathrm{d}\mathbf{r}'\rho(\mathbf{r}')w[|\,\mathbf{r}-\mathbf{r}'\,|;\bar{\rho}(\mathbf{r})] \tag{16}$$

and $w(\mathbf{r})$ is uniquely obtained from requirement (13)

$$c^{(2)}(\mathbf{r}_1,\mathbf{r}_2;[\rho])|_{\rho(r)=\rho} = \frac{\delta c^{(1)}(\mathbf{r}_1;[\rho])}{\delta\rho(\mathbf{r}_2)}\bigg|_{\rho(r)=\rho}. \tag{17}$$

Once $w(r)$ is determined, all higher-order CF's may be calculated via (13).

The results of the different methods will be presented in r space; this was done especially with respect to the SA and its improvements: there, the CF's are directly obtained as functions of r. Comparison in q space would require the determination of $\hat{c}^{(3)}(q,q',q'')$ via FT of $h^{(3)}(r,s,t)$; then Eq. (2) would be used, a calculation which (i) has turned out to be extremely time consuming since we need $h^{(3)}(r,s,t)$ on a large and fine three-dimensional grid and (ii) only limited accuracy for the results can be guaranteed especially for small values of q, q', and q''. In contrast, a high degree of accuracy of the FT of (2) for the other three methods (BHP, KR, and DA) can be guaranteed since the integrands may be extended sufficiently far in q space with only a moderate additional computational effort. Although parametrization of simulation data for $h^{(2)}(r)$ and $c^{(2)}(r)$ exist [20], we have used in this contribution for these two functions the analytical expressions [19,27]. This was done in an effort to guarantee internal consistency of this study, since in the present form the KR method is formulated only in the PY approximation: this should affect the main results only marginally since this study has a *comparative* character.

III. RESULTS

All calculations have been done on a VP50-EX computer. In order to give to the reader an idea of how time consuming the calculations may be, the description of the most "expensive" parts of the respective algorithm and the required CPU times are compiled in Table I.

TABLE I. Required CPU time for the determination of the TDF with different methods (in CPU minutes on a VP-50).

$A_l(r,s)$	210	min
$\tau_1(r,s,t)$	10	min
$\tau_2(r,s,t)$	300	min
Determination of TDF for $\sim$ 100 000 configurations	520	min
Solution of (10)	0.1	min
$\hat{c}^{(3)}_{\mathrm{BHP}}(q_1,q_2,\,|\,\mathbf{q}_1+\mathbf{q}_2\,|)$ (A5)	40	min
FT consisting of Legendre transformation (A2) and radial integration (A3)	2	min
Determination of TDF for $\sim$ 200 configurations	42	min
$c^{(3)}$ (analytic expression KR or DA)	~ 0	min
FT consisting of Legendre transformation (A2) and radial integration (A3)	31	min
Determination of TDF for $\sim$ 400 configurations	31	min

A. Angular dependence

In a first step we have compared the results of the four above-mentioned methods for two different systems, characterized by $\eta = 0.3$ and 0.45, considering for both cases six different triplet configurations, keeping two of the sides fixed and varying the enclosed angle. These configurations are rather general ones with at most one direct contact between the spheres (i.e., not too close structures) and are characterized by different r and s values, letting t range from $|r - s|$ to $(r + s)$ (i.e., letting $\cos\vartheta$ range between +1 and -1, where ϑ is the angle between r and s). The isosceles triangles are characterized by the (r, s) pairs (1.5, 1.5), (2.3, 2.3), and (3.0, 3.0), whereas the general triangles are described by the (r, s) values of (2.8, 1.5), (3.0, 2.0), and (4.0, 2.5). Although $g^{(3)}(r, s, t)$ is a direct measure of the probability to find three particles forming a triangle configuration (r, s, t), we rather depict $h^{(3)}(r, s, t)$. This was done to emphasize those features that *do* differ in the different approaches [the h's in (4) are for *all* methods the same]. We would like to take the occasion to warn the reader that representation of $h^{(3)}$ might cause some misleading conclusions when looking at the figures: (i) the maximum value of $h^{(3)}$ is not directly related to the packing fraction (as we know it intuitively from the pair case) and (ii) the deviation of $h^{(3)}$ from zero for stretched configurations $(\cos\vartheta \sim -1)$ is compensated by the added h's so that finally $g^{(3)}$ tends towards 1. Concerning the core condi-

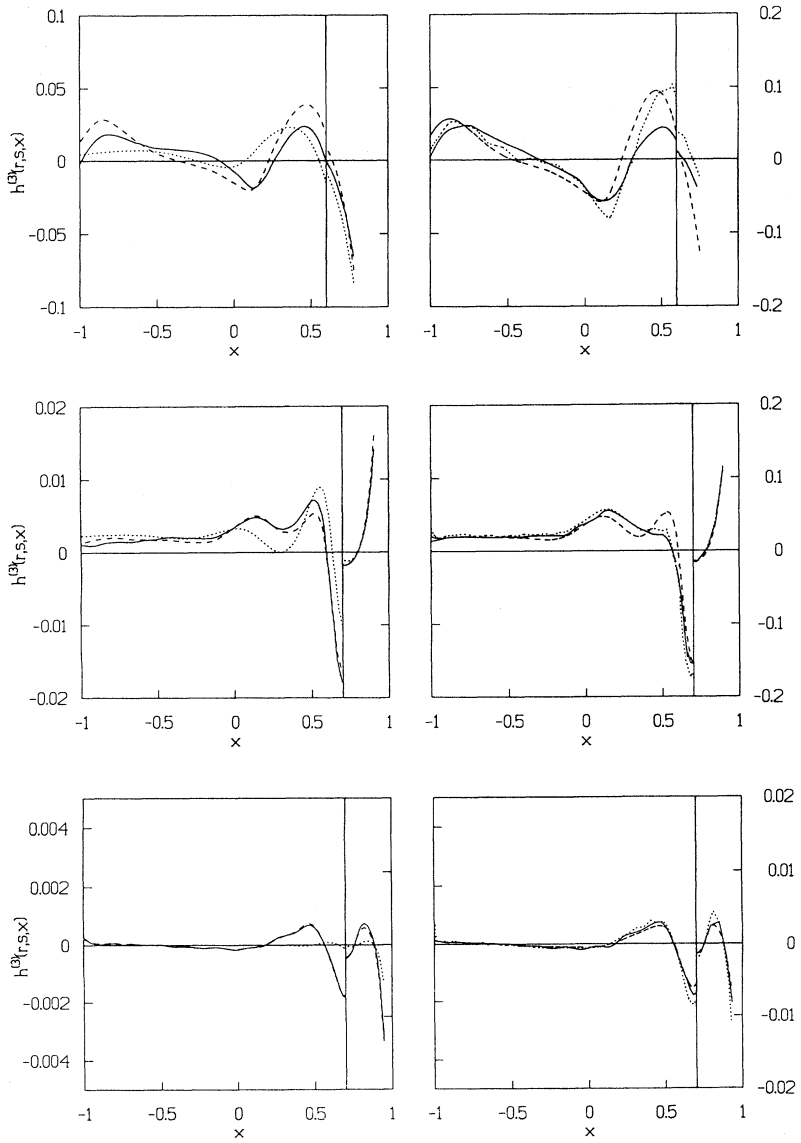

FIG. 1. $h^{(3)}(r, s, x)$, $x = \cos\vartheta$, as a function of x (abscissa) for η=0.3 and the following isosceles configurations (r, s): top (1.5, 1.5), middle (2.3, 2.3), and bottom (3.0, 3.0). The scales of the different x ranges ([-1, 0.7/0.8] and [0.7/0.8, 1], respectively) are found on the left (right) of the respective panels. Symbols: (i) left column: (···) SA, (– –) SA1, and (_____) SA2; (ii) right column: (···) KR, (– –) DA, and (_____) BHP.

tion [i.e., $g^{(3)}(r,s,t) = 0$ for at least one of the arguments being less than 1] we find for BHP, KR, and DA satisfactory results within numerical accuracy (1–2 % of the value at contact). The results are presented in Figs. 1–4.

Let us first discuss a more global comparison and postpone discussions of specific characteristics of the respective methods. We also neglect for the moment the sometimes striking disagreement of the pure SA with the other methods and discuss that later. As may be seen from Figs. 1–4 good agreement—and this is independent of the triangle size—is found for the degenerate configurations at $x \sim 1$, i.e., near contact. Differences in the results then become visible as the triangles spread out, i.e., as x decreases. However, we have to point out that a different scale for $x \in$ [-1, 0.8/0.7] and $x \in$ [0.8/0.7, 1] (differences by a factor of 2 to 10) "blows up" differences in $h^{(3)}$: in this region $h^{(3)}$ has decreased already sufficiently and would contribute only marginally, e.g., in thermodynamic calculations. Concerning the comparison KR, DA, and BHP, a *slight* increase in the difference between the results is observed for shorter distances and higher packing fractions. In the comparison of SA1 and SA2 we find in general very good agreement, except for short distance cases at low η's.

Differences of the respective results near and at the contact of a few configurations are explained as follows: in these configurations the contact value $h^{(3)}(r,s,|\,r-s\,|)$ varies rapidly with r and s; hence different methods will reproduce these changes in rather different ways. Inspection of neighboring configurations that differ in r and/or s by one grid-step size shows that the usual good agreement in encountered again [comparing this situation to the pair case, we also know that different liquid-state theories yield rather different results at or near the contact,

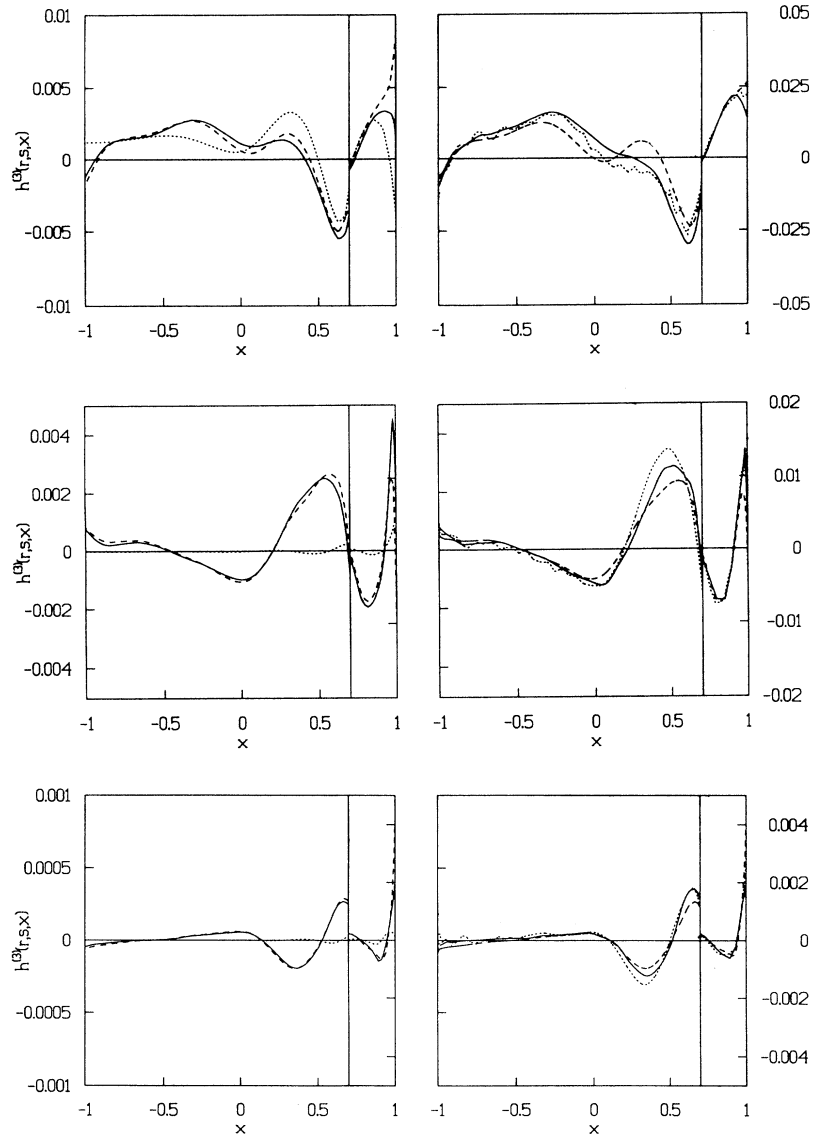

FIG. 2. $h^{(3)}(r,s,x)$, $x = \cos\vartheta$, as a function of x (abscissa) for η=0.3 and the following general configurations (r, s): top (2.8, 1.5), middle (3.0, 2.0), and bottom (4.0, 2.5). Scales and symbols as in Fig. 1.

i.e., in the region where $g(r)$ drops very rapidly].

While the above discussion was a rather general one, we now want to work out specific features of the different methods: the easiest judgement can be done on the SA, which is obviously the most inadequate approximation for $h^{(3)}$ and sometimes does not even nearly contain characteristic information about the triplet structure: often the SA results are out of phase compared to the rather qualitatively coherent picture represented by the other methods and oscillations are in most cases too weak. Hence we may conclude that the SA is a definitively inadequate method to describe the triplet structure of a liquid. The failure of the SA originates from the fact that the influence of correlations of other particles to a given triplet configuration are neglected; these influences may be taken into account via τ_1 and τ_2. However, we have to admit that from our results we could not find a clear tendency how further particles influence the triplet structure: no distinct dependence on the density nor on the geometrical configuration could be observed. In a direct comparison of the DF-based methods (KR and DA) we find the following: in the region $0.7 \leq x \leq 1$ agreement is very good (except for the cases near or at contact, as discussed above). In the x region $[-1, 0.7]$, the agreement is a rather qualitative one: obviously the level where the WDA is introduced *does* have a distinct influence on the triplet structure. Therefore this study also does not give us the possibility to decide which of the DF-based methods is the definitively superior one; only computer simulation results could give a definite answer. Concerning the SA and its improvements we should expect that if we consider the sequence SA-SA1-SA2 for a given triangle configuration (r, s, t), the values of $h^{(3)}(r, s, t)$ should—if the expansion (6) is convergent—tend towards the "true"

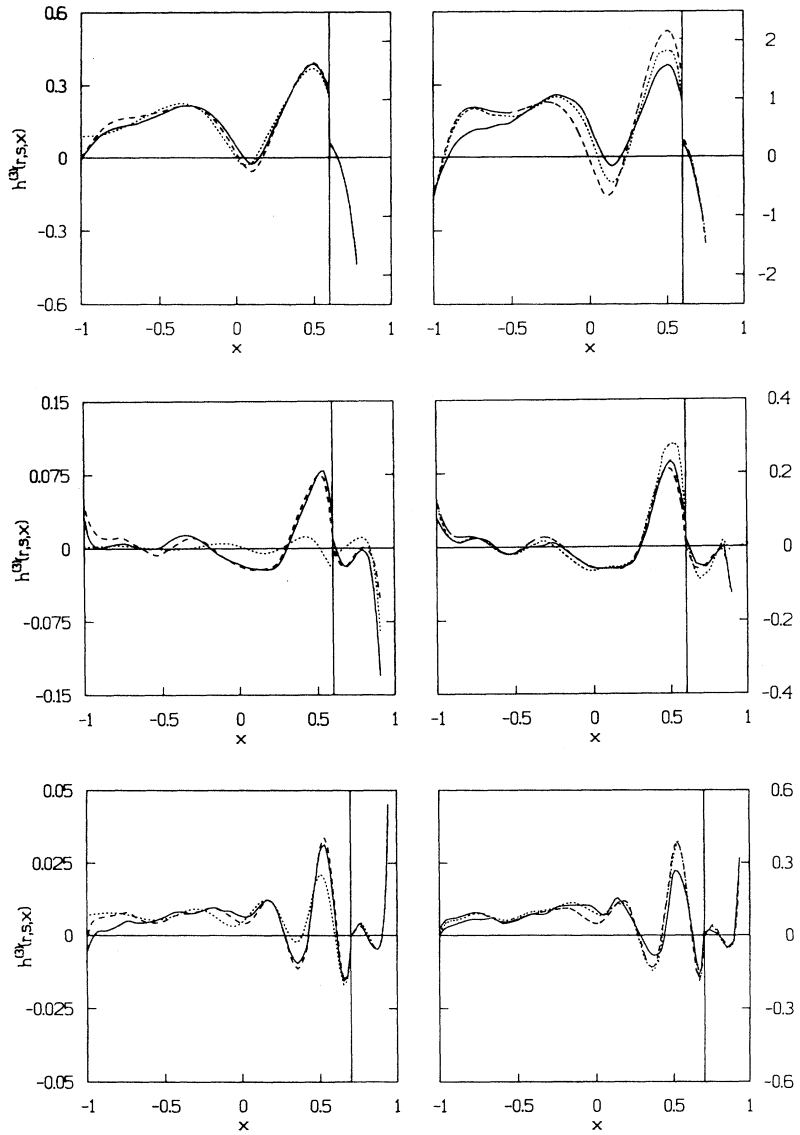

FIG. 3. $h^{(3)}(r, s, x)$, $x = \cos\vartheta$, as a function of x (abscissa) for η=0.45 and the following isosceles configurations (r, s): top (1.5, 1.5), middle (2.3, 2.3), and bottom (3.0, 3.0). Scales and symbols as in Fig. 1.

value of this function (of course, we do not know this function exactly). Although by including τ_1 and τ_2 a net improvement over the SA is clearly visible, we do not dare say that *in general* SA2 will be better than SA1, or, equivalently, that SA2 values lie nearer to the true results than those obtained from SA1. On the other hand, inclusion of $\tau_3(r,s,t)$ in (6), which might give us a more definite answer to this question, is completely hopeless. Finally, the results of the BHP method nicely fit into this rather coherent qualitative picture which we obtain from the different methods treated here. If quantitative differences between the methods occur, they are observed in those regions where $h^{(3)}(r,s,t)$ has decreased sufficiently. All these observations can directly be transferred to the observable $g^{(3)}(r,s,t)$, which differs, according to (4), only by adding the functions $h^{(2)}$, which in turn are for *all* theories the same.

B. Radial dependence

For the study of the radial dependence of our results we have chosen two types of triangle configurations $(r,s,x=\cos\vartheta)$, where ϑ denotes the angle between r and s: isosceles triangles (r,r,x), r ranging from 1 to 3, using three different x values (0.5, 0, −0.5) and general triangles $(r,2r,x)$, r ranging again from 1 to 3 and x being −0.5, 0, and 0.5. These configurations have been considered for the two packing fractions of 0.3 and 0.45. The results are depicted in Figs. 5–8. We observe that $h^{(3)}$ decreases very rapidly as the configurations spread out (the scaling factors used in Figs. 5–8 for the r ranges [1, 1.3] and [1.3, 3] differ by a factor 20–60; this fact has to be taken into account when making quantitative comparisons; this holds especially for the range [1.3, 3], where remarkable difference of the results are observed).

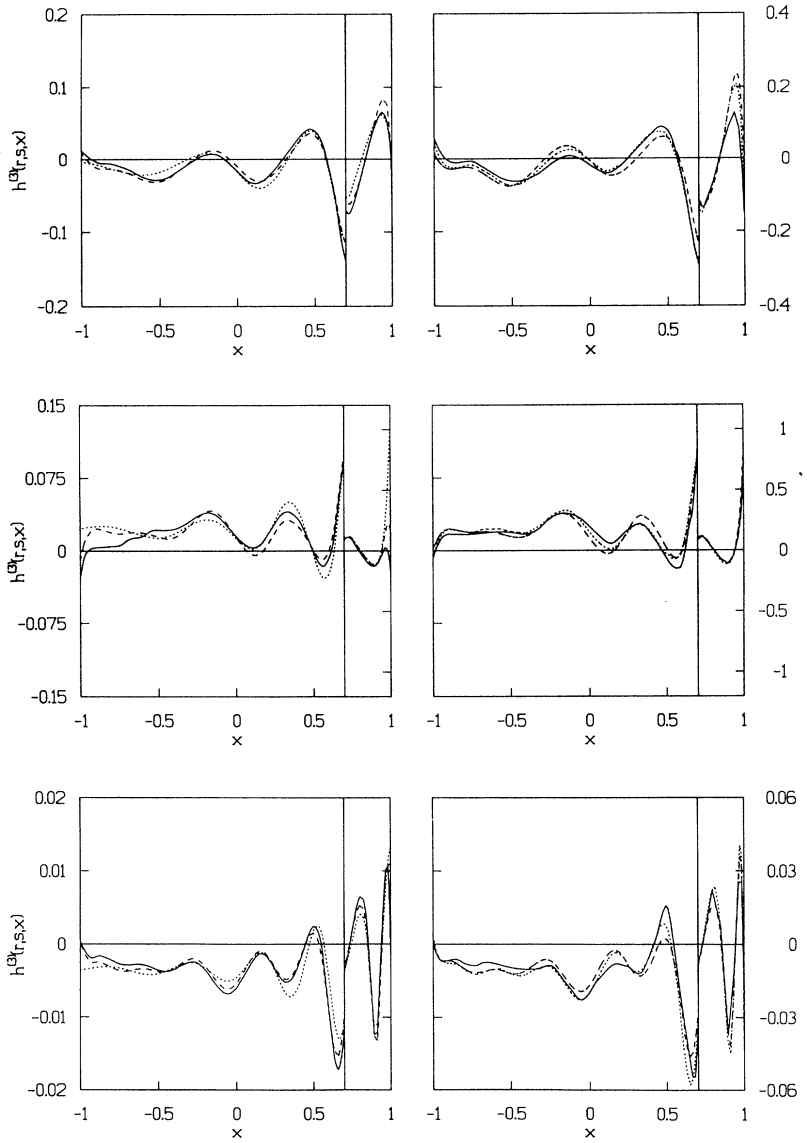

FIG. 4. $h^{(3)}(r,s,x)$, $x=\cos\vartheta$, as a function of x (abscissa) for η=0.45 and the following general configurations $(r,\ s)$: top (2.8, 1.5), middle (3.0, 2.0), and bottom (4.0, 2.5). Scales and symbols as in Fig. 1.

In the interesting range [1, 1.3] a satisfactory quantitative agreement is observed. SA1 and SA2 are in the r range [1, 1.3] in good agreement, except for some configurations near contact where differences of less than 10% are observed. In the comparison of KR, BHP, and DA, the DA method tends to differ in several configurations by about 15% from the other two approximations, whereas KR and BHP agree in all configurations studied rather well. In the less interesting region ($r \in [1.3, 3]$), where $h^{(3)}$ has dropped sufficiently, we observe that the different approaches are in general in phase, i.e., we observe qualitative agreement. The encountered differences are in general larger for x=0.5, while agreement is considerably better for the obtuse angle ($x = -0.5$). Differences between the methods typically range from 20% ($x = 0.5$) to less than 10% ($x = -0.5$). Again, the pure superposition approximation produces results which differ in most cases strongly from the other data.

C. Rolling contact

We now consider configurations of "rolling contact [5]," i.e., configurations where two spheres are separated by a distance s and the third one moves along the surface of one of the two spheres (i.e., at a distance r=1); in the initial configuration, the third sphere is in direct contact with the other two spheres, defining a minimum angle $\vartheta_{\min}$ which is enclosed by r (=1) and s (hence $\cos\vartheta_{\min} = s/2$). The third sphere then moves, as described above, until a stretched configuration is obtained. Such configurations have been studied recently by Attard [5] in HS systems, using his "PY3" method; he obtains

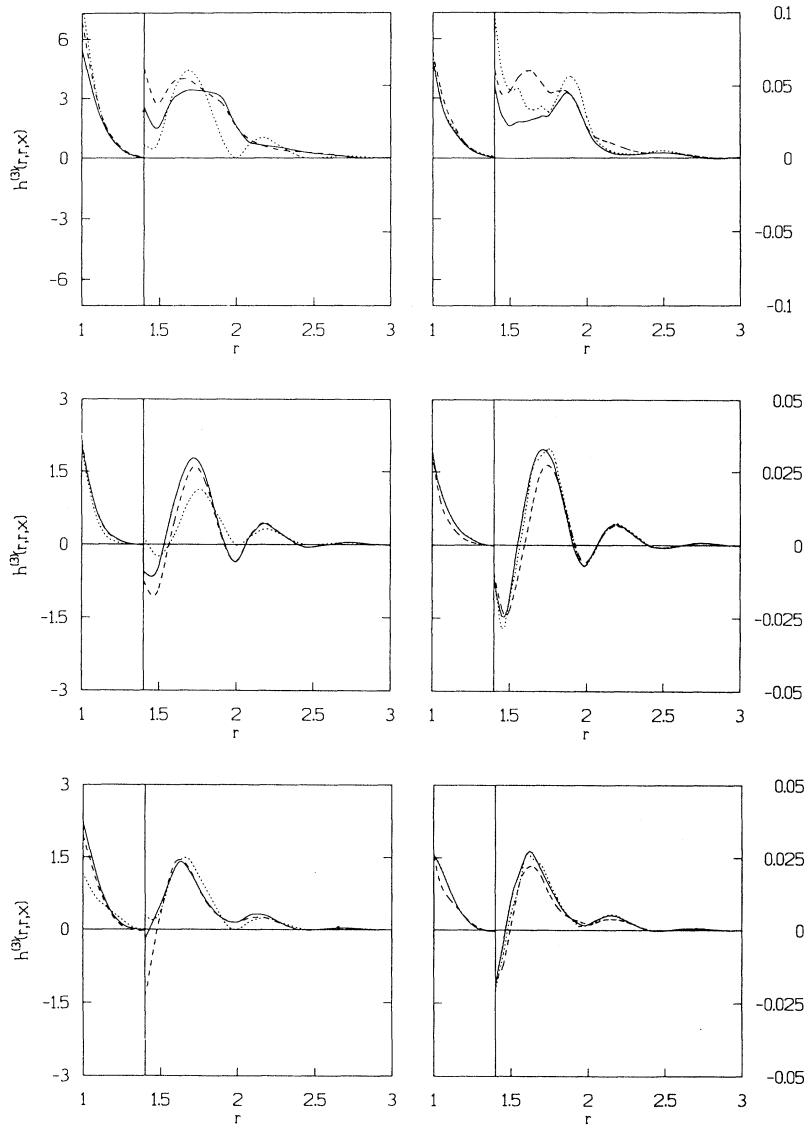

FIG. 5. $h^{(3)}(r, r, x)$, $x = \cos\vartheta$, as a function of r for η=0.3 for three different x values: 0.5 (top), 0.0 (middle), and −0.5 (bottom). Symbols and labeling as in Fig. 1.

excellent agreement (practically identical results) with (not too recent) computer simulations [18] for a system characterized by $\eta = 0.8368\pi/6$. Our results are depicted in Fig. 9 for four different s values, where we compare data obtained from Attard's method [31] with SA2 and KR results; here we use a packing fraction $\eta = 0.7\pi/6$. The restriction to these two methods was done in an effort to limit the number of results; the data presented in the two preceding subsections should give the reader an idea by what extent BHP and DA differ from the other two approximations. Although again the qualitative behavior is quite similar for all methods, substantial quantitative differences occur especially for the smaller s values. While for larger distances s these differences become of the order of magnitude as encountered in the previous parts of the study, the situation is different for closed configurations: the smallest s values represent triangle configurations where the spheres form very close packed structures; substantial differences for the $h^{(3)}$ results are observed in these cases. This may remind us of the pair case: PY and (e.g.) HNC $g^{(2)}(r)$ also differ for x values near contact substantially (especially for higher packing fractions). Hence our results indicate that the sensitivity of the contact value of an n-particle DF is also observed in the triplet case.

IV. CONCLUSIONS

In this study we have presented numerical results of the TDF obtained from several methods which have been proposed during the past years. The system we have taken into account is a fluid of hard spheres. Due to the lack of extensive and recent results of computer ex-

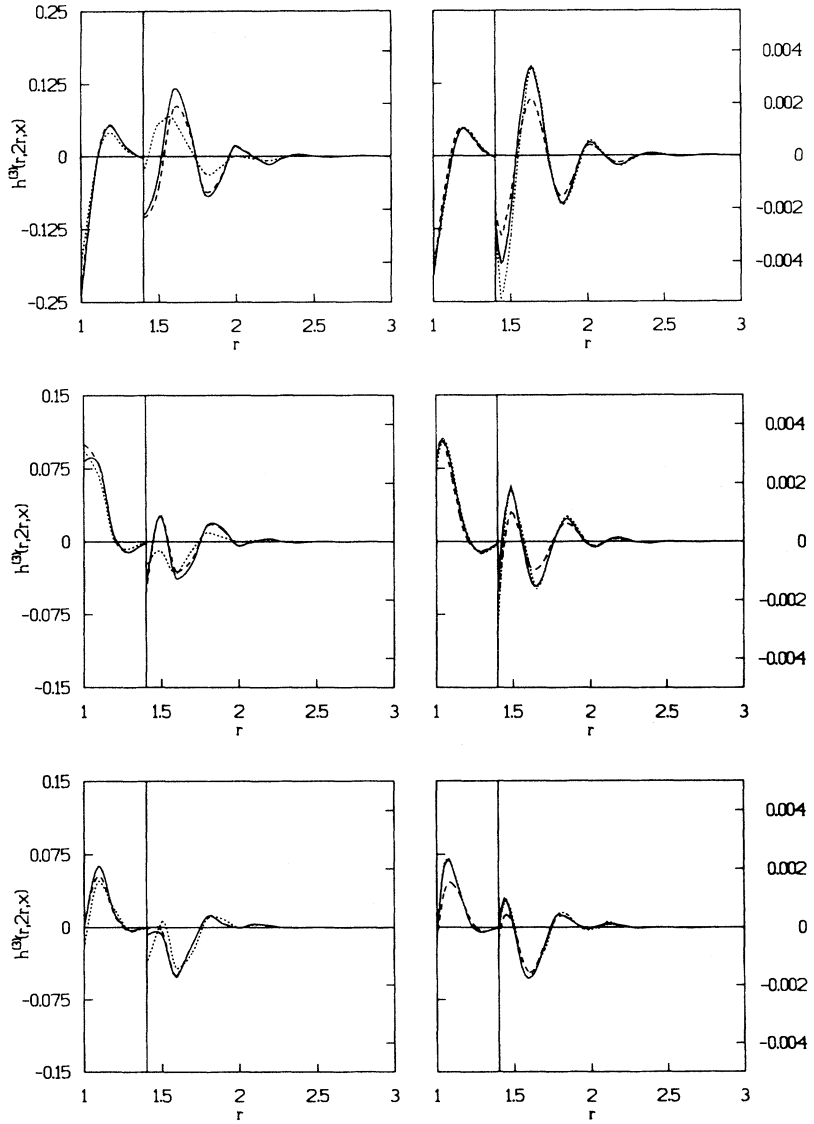

FIG. 6. $h^{(3)}(r, 2r, x)$, $x = \cos\vartheta$, as a function of r for η=0.3 for three different x values: 0.5 (top), 0.0 (middle), and −0.5 (bottom). Symbols and labeling as in Fig. 1.

periment in r space, we have compared these methods among themselves, which allows us to draw conclusions of how consistent present-day methods for the determination of triplet correlation functions are. We find, despite the different origins of these methods, a rather coherent picture, i.e., we find for not extremely close-packed triplet configurations that in general rather good *qualitative* agreement is encountered. The *quantitative* agreement is found to be very good for larger distances; disagreement between the methods increases as we shorten the distances and we finally encounter substantial differences in those configurations where all three spheres are in very close contact. In general, agreement is slightly worse for higher packing fractions. Finally, in all cases the Kirkwood SA is found to be an inadequate approximation for $h^{(3)}$ which does not contain characteristic informations about the triplet structure; hence we strongly advise not using it.

ACKNOWLEDGMENTS

The authors are indebted to Dr. Giorgio Pastore (Trieste) for leaving them a code for the BHP method [28]. Special thanks is due to Dr. P. Attard (Canberra) for providing unpublished data [31]. This work was supported by the Österreichische Forschungsfonds under Projects Nos. P7618-TEC and P8912-PHY.

APPENDIX: NUMERICAL DETAILS

If we assume the definition of the FT's (3) and let ϑ (ϕ) be the angle between $\mathbf{r}$ and $\mathbf{r}'$ ($\mathbf{q}$ and $\mathbf{q}'$) and $x = \cos\vartheta$, $y = \cos\phi$, then

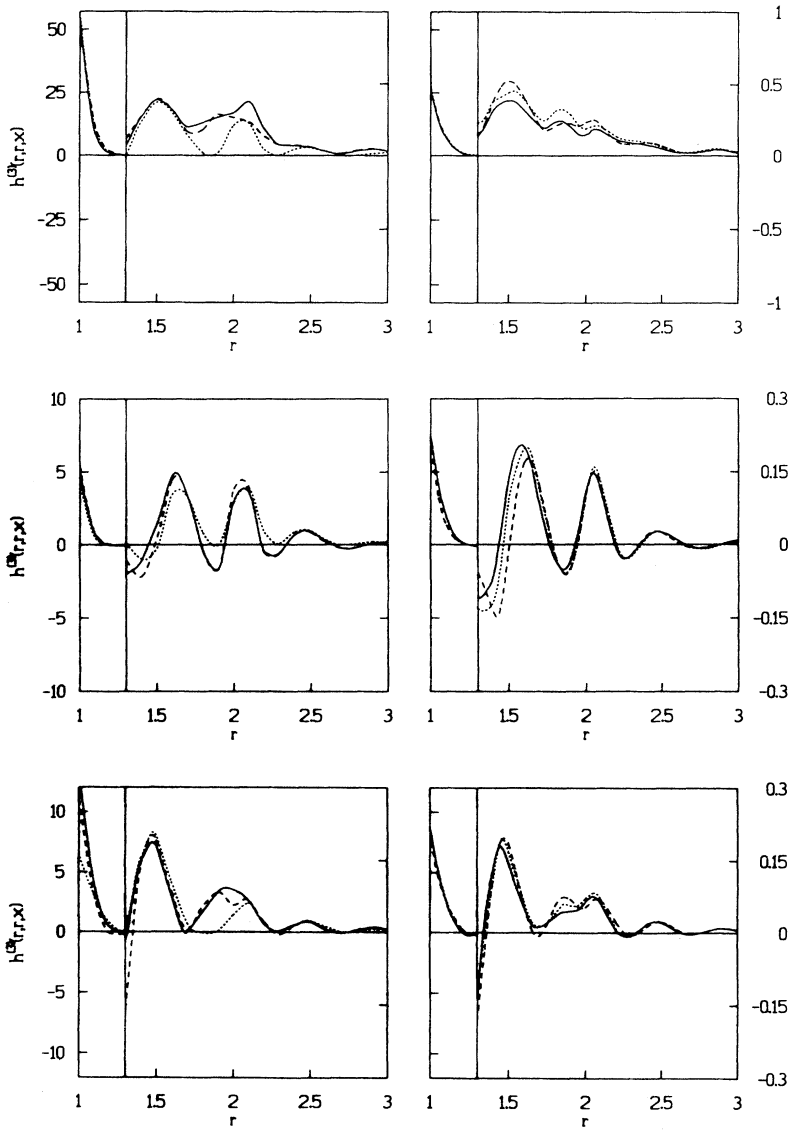

FIG. 7. $h^{(3)}(r,r,x)$, $x = \cos\vartheta$, as a function of r for η=0.45 for three different x values: 0.5 (top), 0.0 (middle), and -0.5 (bottom). Symbols and labeling as in Fig. 1.

$$f(\mathbf{r},\mathbf{r}') = f(r,r',x) = \sum_l f_l(r,r')P_l(x), \tag{A1}$$

$$\hat{f}(\mathbf{q},\mathbf{q}') = \hat{f}(q,q',y) = \sum_l \hat{f}_l(q,q')P_l(y), \tag{A2}$$

where

$$f_l(r,r') = \frac{4}{(2\pi)^4}(-1)^l \times \int_0^\infty dq_1 dq_2 q_1^2 q_2^2 j_l(q_1 r) j_l(q_2' r) \hat{f}_l(q_1,q_2), \tag{A3}$$

$$\hat{f}_l(q,q') = 16\pi^2(-1)^l \times \int_0^\infty dr_1 dr_2 r_1^2 r_2^2 j_l(r_1 q) j_l(r_2 q') f_l(r_1,r_2). \tag{A4}$$

The $j_l(x)$ are the standard spherical Bessel functions.

We now turn to the numerical parameters of the different methods. (i) In the SA and its improvements (SA1 and SA2) the diagrams representing $\tau_1(r,s,t)$ and $\tau_2(r,s,t)$ are calculated using the well-known Legendre-expansion technique [26]. Although tables exist in Ref. [2] how to determine this coefficients, we want to take this occasion to point out an obvious misprint in

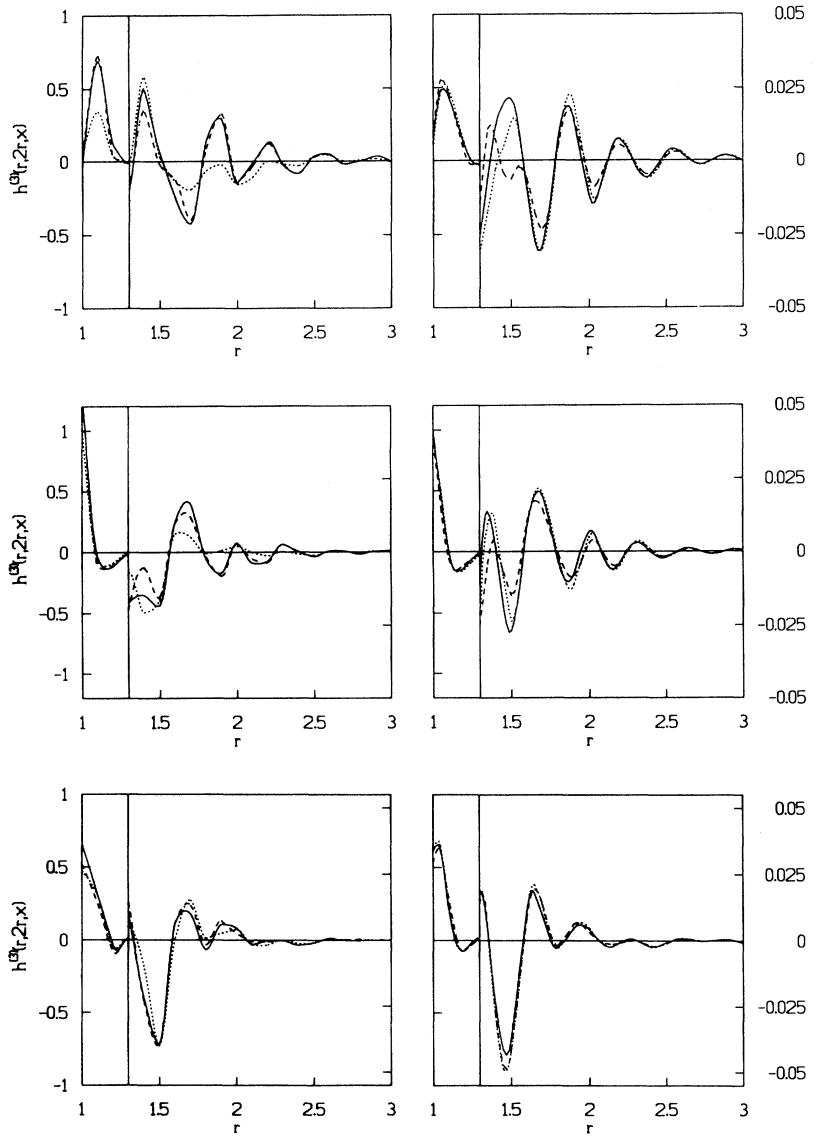

FIG. 8. $h^{(3)}(r,2r,x)$, $x = \cos\vartheta$, as a function of r for η=0.45 for three different x values: 0.5 (top), 0.0 (middle), and –0.5 (bottom). Symbols and labeling as in Fig. 1.

these papers: there the expression for the seven-bond diagram is obviously not symmetric in r and s (as it, of course, should be), whereas our formula fulfills this requirement. The prescription of how to evaluate the diagrams (7) and (8) using the Legendre-expansion technique is summarized in Table II, the expansion coefficients are presented in Table III. Table III also contains the actual numerical parameters used in our calculations, i.e., both the upper summation limits of the expressions as well as the grid and the mesh size on which these coefficients and hence τ_1 and τ_2 were determined. The respective parameters (both the summation index as well as the range of the grid) have found to be sufficient to guarantee an accuracy of 1–2 % (on the average) of the final results. The diagrams τ_1 and τ_2 have been calculated on a three-dimensional grid (r, s, t), each side extending over six HS diameters (beyond the core) containing 61 grid points. The seven-bond diagram has been evaluated on a 36 × 36 × 36 grid, extending over 3.5 HS diameters (beyond the core); this reduction in distance is both due to numerical reasons (summation over five indices is extremely time consuming) and to the fact that $H_{lmnpq}(r, s)$ decreases rapidly in distance.

(ii) In the BHP method, $\hat{t}(q)$ was determined numerically, as described in the Appendix of Ref. [4], from solving the FT of Eq. (10); $\hat{t}(q)$ then served to construct $\hat{c}(\mathbf{q}, \mathbf{q}')$ via

$$\hat{c}(\mathbf{q}, \mathbf{q}') = \frac{1}{(2\pi)^3} \int \hat{t}(q'')\, \hat{t}(|\, \mathbf{q} - \mathbf{q}''\,|)\, \hat{t}(|\, \mathbf{q}' + \mathbf{q}''\,|) d\mathbf{q}''$$

$$= \hat{c}(q, q', y) = \sum_{l=0}^{\infty} \hat{c}_l(q, q') P_l(y). \qquad \text{(A5)}$$

$\hat{c}_l(q, q')$ was determined on a 200 × 200 grid in (q, q') space with a mesh size of 0.2; the actual summation in (A5) was performed for $l = 0$ to 31.

$h^{(3)}(r, s, t)$ was obtained both for BHP and the DF-based methods via a FT of (2): the first three summands are transformed directly (i.e., *not* numerically) into products of $h(r)$'s of appropriate r arguments, and the remaining last term is transformed numerically using relation (A3).

Of course $h^{(3)}(r, s, x)$ is discontinuous for HS along the contact, but it turns out that the first three terms of (2), i.e., the products of h's, represent the major part of this discontinuity so that the FT of the last term is a rather well-behaved function across the contact.

(iii) In both DF-based methods the radial integrations (A3) extend over 400 grid points ($\Delta q = \Delta q' = 0.1$). The discrete Legendre transformation proposed by Attard [5] includes 64 angular nodes. $h^{(3)}(\mathbf{r}, \mathbf{r}')$ was then obtained as described above.

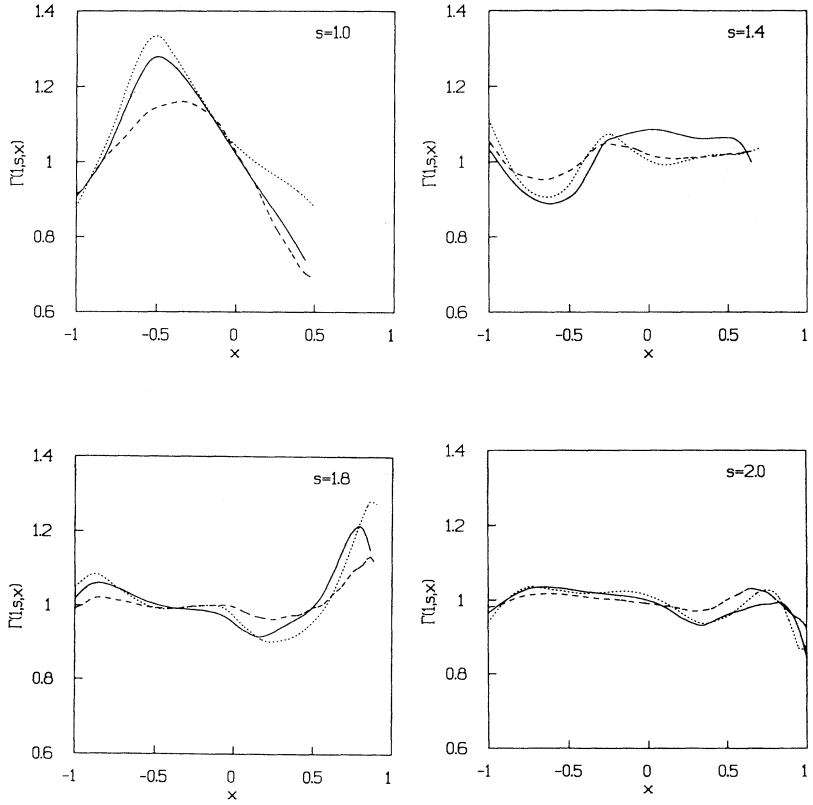

FIG. 9. $\Gamma(1, s, x) = g^{(3)}(1, s, x)/[g(1)g(s)g(t)]$, $x = \cos\vartheta$, and $t^2 = 1 + s^2 - 2sx$ as a function of x for $\eta = 0.7\pi/6$ and different s values as indicated. Symbols: (_____) PY3 (Ref. [31]), (· · ·) SA2, and (– –) KR.

TABLE II. Legendre expansion of the diagrams representing $\tau_1(r,s,t)$ (7) and $\tau_2(r,s,t)$ (8). ϑ is the angle between r and s. The actual upper limits of the different summations and the (r,s) ranges over which the diagrams have been calculated may be seen from the respective columns of Table III. Θ are the Legendre functions as defined in Table III.

$f(t)$	=	$\sum_{l=0}^{\infty} A_l(r,s) P_l(\cos\vartheta)$
Three-bond diagram	=	$4\pi \sum_{l=0}^{\infty} B_l(r,s) \frac{1}{2l+1} P_l(\cos\theta)$
Five-bond diagram	=	$16\pi^2 \sum_{l=0}^{\infty} E_l(r,s) \frac{1}{(2l+1)^2} P_l(\cos\vartheta)$
Six-bond diagram	=	$16\pi^2 \sum_{l,m,n=0}^{\infty} \epsilon_{lmn} F_{lmn}(r,s) \frac{1}{2m+1} P_n(\cos\vartheta)$
Seven-bond diagram	=	$64\pi^2 \sum_{\substack{l,m,n,p,q=0 \\ \min\{mnq\}}}^{\infty} H_{lmnpq}(r,s) \frac{1}{\sqrt{2l+1}(2m+1)(2n+1)\sqrt{2p+1}(2q+1)}$
		$\times \sum_{j=-\min\{mnq\}} \Theta_{m\ -j}(\cos\vartheta)\Theta_{q\ -j}(\cos\vartheta)\gamma^j_{npq}\gamma^j_{nlm}$

TABLE III. Expressions of how to determine the Legendre expansion coefficients of the diagrams representing $\tau_1(r,s,t)$ (7) and $\tau_2(r,s,t)$ (8). f stands for $h^{(2)}(r)$. The second column contains the upper limits of the indices $(l,m,...)$ of the coefficients used in this calculation. Columns three and four contain the range in r, s, and t (column three) and the mesh size (column four) of the grid on which the coefficients were calculated (both in units of the HS diameter). The integrations in the range [0, 1] [where $h^{(2)}(r) = -1$] were performed—wherever possible—analytically.

$A_l(r,s) = (l+\frac{1}{2}) \int_0^{\pi} d\vartheta \sin\vartheta P_l(\cos\vartheta) f(t)$	30	[1, 7]	0.05
$B_l(r,s) = \int_0^{\infty} dt\, t^2 f(t) A_l(r,t) A_l(s,t)$	30	[1, 7]	0.05
$E_l(r,s) = \int_0^{\infty} dt\, t^2 f(t) A_l(r,t) B_l(s,t)$	14	[1, 7]	0.10
$F_{lmn}(r,s) = \int_0^{\infty} dt\, t^2 f(t) A_l(r,t) B_m(r,t) A_n(s,t)$	14	[1, 7]	0.10
$G_{npq}(t,r,s) = \int_0^{\infty} du\, u^2 f(u) A_n(t,u) A_p(r,u) A_q(s,u)$	14	[1, 4.5]	0.10
$H_{lmnpq}(r,s) = \int_0^{\infty} dt\, t^2 f(t) A_l(r,t) A_m(s,t) G_{npq}(t,r,s)$	14	[1, 4.5]	0.10

$$\epsilon_{lmn} = \tfrac{1}{2} \int_{-1}^{1} dx P_l(x) P_m(x) P_n(x)$$

$$\gamma^j_{npq} = \int_{-1}^{1} dx\, \Theta_{nj}(x) \Theta_{p0}(x) \Theta_{q\ -j}(x)$$

$$\Theta_{lm}(x) = (-1)^m \Theta_{l\ -m}(x) = (-1)^m \sqrt{\tfrac{(2l+1)(l-m)!}{2(l+m)!}} (1-x^2)^{m/2} \tfrac{d^m}{dx^m} P_l(x)$$

[1] G. Stell, Physica **29**, 517 (1963); in *The Equilibrium Theory of Classical Fluids*, edited by H.L. Frisch and J.L. Lebowitz (Benjamin, New York, 1964), pp. 11–171.
[2] A.D.J. Haymet, S.A. Rice, and W.G. Madden, J. Chem. Phys. **74**, 3033 (1981); **75**, 4696 (1981); W.J. McNeil, W.G. Madden, A.D.J. Haymet, and S.A. Rice, *ibid.* **78**, 388 (1983); A.D.J. Haymet, J. Phys. (Paris) Colloq. **46**, C9-27 (1985).
[3] J.-L. Barrat, J.-P. Hansen, and G. Pastore, Phys. Rev. Lett. **58**, 2075 (1987).
[4] J.-L. Barrat, J.-P. Hansen, and G. Pastore, Mol. Phys. **63**, 747 (1988).
[5] P. Attard, J. Chem. Phys. **91**, 3072 (1989); Mol. Phys. **74**, 547 (1991).
[6] P. Attard, J. Chem. Phys. **93**, 7301 (1990); **94**, 6936(E) (1991); **94**, 4471 (1991).
[7] J. Bławzdziewicz, B. Cichocki, and R. Hołyst, Physica A **157**, 857 (1989); J. Bławzdziewicz, B. Cichocki, and G. Szamel, J. Chem. Phys. **91**, 7467 (1989).
[8] Y. Rosenfeld, Phys. Rev. Lett. **63**, 980 (1989); J. Chem. Phys. **89**, 4272 (1988).
[9] Y. Rosenfeld, D. Levesque, and J.-J. Weis, J. Chem. Phys. **92**, 6818 (1990).
[10] E. Kierlik and M.L. Rosinberg, Phys. Rev. A **42**, 3382 (1990).
[11] A.R. Denton and N.W. Ashcroft, Phys. Rev. A **39**, 426 (1989).
[12] A.R. Denton and N.W. Ashcroft, Phys. Rev. A **44**, 1219 (1991).
[13] W.A. Curtin, J. Chem. Phys. **93**, 1919 (1990); W.A. Curtin and N.W. Ashcroft, Phys. Rev. Lett. **59**, 2385 (1987).
[14] J.-P. Hansen and I.R. McDonald, *Theory of Simple Liquids*, 2nd ed. (Academic, London, 1986).
[15] J. Talbot, J.L. Lebowitz, E.M. Waisman, D. Levesque, and J.-J. Weis, J. Chem. Phys. **85**, 2187 (1986).
[16] M. Fushiki, Chem. Phys. Lett. **154**, 77 (1989); M. Fushiki, Mol. Phys. **74**, 307 (1991).
[17] A. Baranyai and D.J. Evans, Phys. Rev. A **40**, 3817 (1989); **42**, 849 (1990).
[18] A. Bellemanns and J. Orban, Chem. Phys. Lett. **2**, 253 (1968).
[19] M.S. Wertheim, Phys. Rev. Lett. **10**, 321 (1963); J. Math. Phys. **5**, 643 (1964); E. Thiele, J. Chem. Phys. **39**, 474 (1963).
[20] L. Verlet and J.-J. Weis, Phys. Rev. A **5**, 939 (1972); D. Henderson and E.W. Grundke, J. Chem. Phys. **63**, 601 (1975).
[21] L.L. Lee, J. Chem. Phys. **60**, 1197 (1974).
[22] R. Abe, Prog. Theor. Phys. **21**, 421 (1959).
[23] E.E. Salpeter, Ann. Phys. (N.Y.) **5**, 183 (1958).
[24] J.G. Kirkwood, J. Chem. Phys. **3**, 300 (1935).
[25] R. Evans, Adv. Phys. **28**, 143 (1979).
[26] J.A. Barker and D. Henderson, J. Chem. Phys. **36**, 2564 (1962); D. Henderson, *ibid.* **46**, 4306 (1967).
[27] W.R. Smith and D. Henderson, Mol. Phys. **19**, 411 (1970); G. Kahl, *ibid.* **67**, 879 (1989).
[28] J.-L. Barrat and G. Pastore (unpublished).
[29] P. Tarazona, Mol. Phys. **52**, 81 (1984); Phys. Rev. A **31**, 2672 (1985).
[30] W.A. Curtin and N.W. Ashcroft, Phys. Rev. A **32**, 2909 (1985).
[31] P. Attard (unpublished).